International Conference on Applied Energy 2019
Aug 12-15, 2019, Västerås, Sweden
Paper ID: 0040

THERMODYNAMIC PERFORMANCE ANALYSIS OF A TRIPLE-PRESSURE ORC - COMPARISON WITH SINGLE-PRESSURE AND DUAL-PRESSURE ORCS

Hao Yu[1,2], Xinli Lu [1,2*], Taidou Wang[1,2], Jiaqi Zhang[1,2], Yuncheng Gu[1,2], Changyou Geng[1,2]

1 Tianjin Geothermal Research and Training Center, Tianjin University, Tianjin 300350, PR China

2 Key Laboratory of Efficient Utilization of Low and Medium Grade Energy, MOE, Tianjin University, Tianjin 300350, PR China

* Corresponding author. Tel.: +86-18522972804, Email address: xinli.lu@tju.edu.cn

ABSTRACT

A triple-pressure organic Rankine cycle (TPORC) using geothermal energy for power generation has been investigated in this paper. The net power output of the TPORC was analyzed by varying the evaporation pressures, pinch temperature differences and degrees of superheat to find the optimum operation conditions of the system. The thermodynamic performance of the TPORC was compared with dual-pressure ORC (DPORC) and single-pressure ORC (SPORC) respectively for the heat source (geofluid) temperature between 135°C and 200°C. The results show that the net power output of the TPORC is higher than that of the DPORC and SPORC when the heat source temperature is low, especially when it is less than 150°C. Thus the TPORC could be a choice for power generation for utilizing medium-low geothermal resources (100°C-150°C) provided that it has a sound techno-economics.

Keywords: Geothermal power generation systems, Single-pressure ORC, Dual-pressure ORC, Triple-pressure ORC.

NONMENCLATURE

Abbreviations	
HP	High-pressure
MP	Medium-pressure
LP	Low-pressure
SPORC	Single-pressure Organic Rankine Cycle
DPORC	Dual-pressure Organic Rankine Cycle
TPORC	Triple-pressure Organic Rankine Cycle
Subscripts	
h	High-pressure stage
m	Medium-pressure stage
l	Low-pressure stage
Symbols	
η	efficiency

1. INTRODUCTION

The global geothermal resources can be roughly divided into five categories: hydrothermal geothermal resources, dry steam geothermal resources, abnormal stratum pressure geothermal resources, magmatic hot dry rock and hot dry rock [1]. The concept of EGS (Enhanced Geothermal System), which includes the earlier concept of HDR (Hot Dry Rock), originated from the Los Alamos National Laboratory (LANL) in the USA. EGS could become a promising energy technology for power generation and considerably reduce the consumption of fossil fuels [2,3].

In terms of utilizing geothermal energy from the EGS efficiently, reducing the temperature difference between the heat resource (geofluid) and working fluid is a commonly used method, such as introducing zeotropic mixture into the ORC systems [4,5]. Kang et al. [6] analyzed the influences of 10 groups of mixtures on the performance of ORC. Shahram et al. [7] established thermodynamic models of three different ORCs to compare their performances of power generation using geothermal energy.

Selection and peer-review under responsibility of the scientific committee of the 11th Int. Conf. on Applied Energy (ICAE2019).
Copyright © 2019 ICAE

The dual-pressure ORC (DPORC) consists of two evaporators at different pressures. The power output gains deriving from the dual pressure configuration are particularly high (up to 29%) at lower geothermal fluid temperatures (100-125°C) [8]. Li et al.[9, 10] studied the optimal cycle parameters for various heat source temperatures by selecting nine pure organic fluids as working fluids and performed a comparative analysis of two turbine layouts. In addition, the thermodynamic performances of the basic, dual-pressure and dual-fluid ORCs and Kalina cycles using geothermal energy for power generation have been analyzed respectively from energy, exergy and exergoeconomic viewpoints [11-13]. When choosing R1233zd as working fluid, the average increasing rate of 20.87% in net power output (W_{net}) brings no economic benefits to the dual pressure system because the electricity production cost (EPC) also increases 12.98% averagely compared to the SPORC [14-16].

Previous studies showed that the DPORC could increase the power output by reducing the exergy loss in evaporation. In this study, a triple-pressure ORC (TPORC) has been investigated to find out whether more evaporation stages will lead to more net power output by comparison with the DPORC and SPORC for heat source temperature between 135 and 200 °C.

2. DESCRIPTION OF THE GEOTHERMAL POWER GENERATION SYSTEMS

Schematics of the SPORC, DPORC and TPORC using geothermal energy for power generation are shown in Fig.1 respectively. Each system can be categorized into three parts based on the types of fluids: the dash (red) lines represent the geothermal water flow path; the heavy (black) lines represent the flow path of the ORC working fluid; the fine (yellow) lines represent the flow path of cooling water.

The schematic diagram of SPORC is shown in Fig.1 (a), and its temperature-entropy diagram is shown in Fig.2 (a). Different from the SPORC, the DPORC (Fig.1 (b)) has high-pressure and low-pressure evaporation processes. After being preheated to the low-pressure saturated liquid (state 5_l), the saturated working fluids are divided into two streams: one stream directly flows into the LP-Evaporator where it is heated by the geothermal water to the superheated state (state 1_l) and then goes to the LP-Turbine for power generation; the other stream is pumped to the HP-Evaporator (5_l-7) and then it passes through the HP-Preheater and HP-Evaporator and finally becomes the high-pressure superheated vapor (state 1_h) before it enters the HP-Turbine. The temperature-entropy diagram of DPORC is shown in Fig.2 (b).

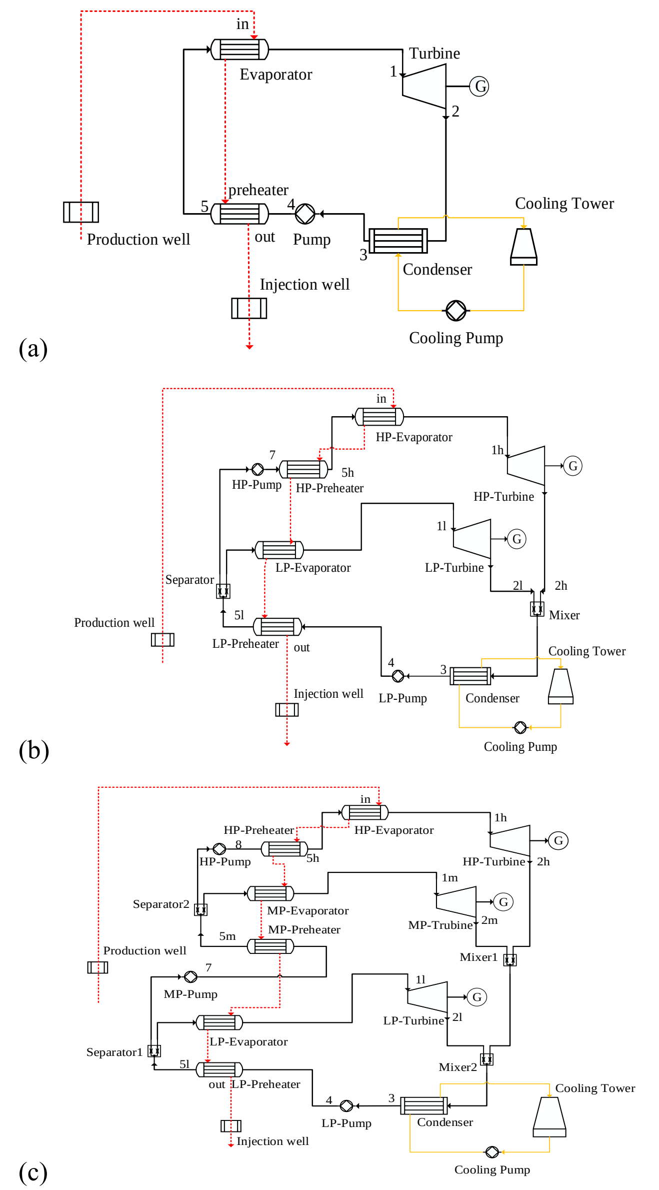

Fig.1. Schematic diagrams of three geothermal power generation systems: (a) SPORC; (b) DPORC; (c) TPORC.

In the TPORC system (Fig.1 (c)), there are three different pressure (high-pressure, medium-pressure, low-pressure) evaporation processes. The working fluid is divided into two streams in the Separator 1: one is heated to the low-pressure superheated vapor (state 1_l); the other is pumped to the medium-pressure (5_l-7) and is heated to the saturated liquid (state 5_m) in the MP-Preheater. It is then flows into the Separator 2 where it is again divided into two parts. One stream passes the MP-Evaporator and becomes superheated vapor (state 1_m) that goes to the MP-Turbine; the other is pumped to a higher pressure condition (state 8) and

Copyright © 2019 ICAE

passes through the HP-Preheater and the HP-Evaporator, becoming superheated state (state 1_h) before it enters the HP-Turbine. The temperature-entropy diagram of TPORC is shown in Fig.2 (c).

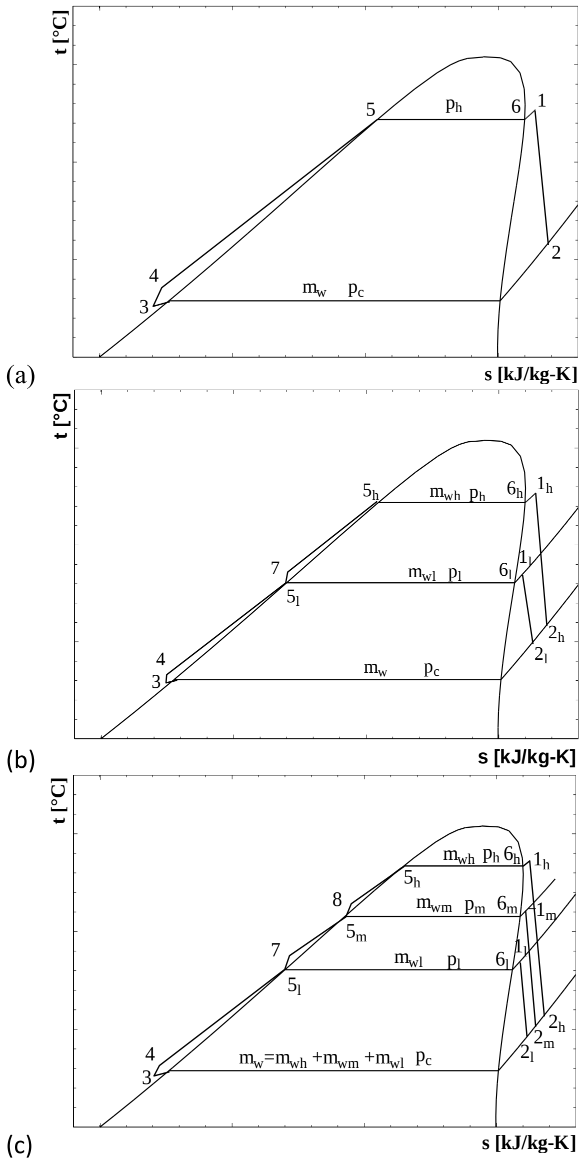

Fig.2. T-S diagrams of three geothermal power generation cycles: (a) SPORC; (b) DPORC; (c) TPORC.

3. BRIEF DESCRIPTION OF THE THERMODYNAMIC MODELS

Detailed thermodynamic models of the systems are not shown here due to the length limit of the article. Some assumptions used in the models are listed here, as follows:

(1) Heat and pressure loss in the systems were neglected;

(2) Pinch temperature difference (T_e) varied from 5 to 15°C;

(3) Degree of superheat (d_t) varied from 2 to 12°C;

(4) Ambient temperature and pressure: t_0=20°C, p_0=1bar;

(5) HP-Evaporator pressure (p_h) range: 5-30 bar;

(6) MP-Evaporator pressure (p_m) range: 3-28 bar;

(7) LP-Evaporator pressure (p_l) range: 2 -20 bar.

Simulation models were built using Engineering Equation Solver (EES). The ORC working fluid used for the simulation is R245fa. The governing equations were formulated based on mass and energy balances. The net power output were chosen as an objective function. The power consumption of geothermal water, cooling water and fan power consumption of the cooling tower have been taken into account for the net power output calculation.

4. THERMODYNAMIC ANALYSIS AND RESULTS

4.1 Parametric study of the TPORC

The net power output was calculated for different thermodynamic parameters. Due to the length limit of this article, the calculation results of SPORC and DPORC are not presented here.

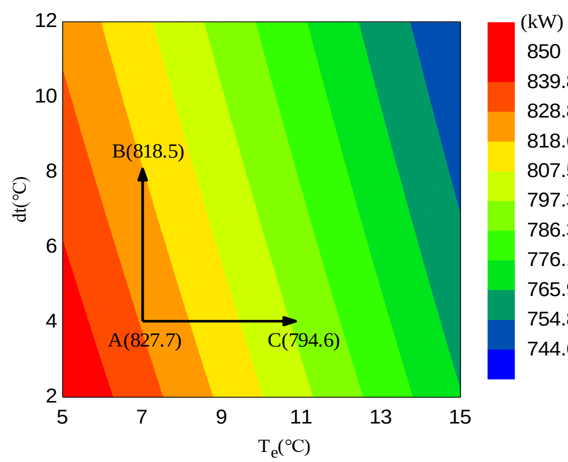

Fig.3. The net power output variations of the TPORC with respect to the pinch temperature difference (T_e) and the degree of superheat (d_t). (p_h = 25 bar, p_m = 16 bar, p_l = 8 bar)

Fig.3. shows the net power output variations of the TPORC with respect to the pinch temperature difference (T_e) and the degree of superheat (d_t) under the condition that p_h = 25 bar, p_m = 16 bar, and p_l = 8 bar. When d_t is constant, the increase of T_e, will result in a decrease of the net power output; when T_e is constant, the higher the d_t, the less the net power output. Lowering pinch temperature difference and the degree of superheat will lead to more power generation. It is also seen from Fig.3 that the decrease of the net power output along A-C is greater than that along A-B, indicating that the pinch

Copyright © 2019 ICAE

temperature difference has greater influence than the degree of superheat on the net power output.

understand why the optimum value of p_h is on the upper boundary (as shown in Fig. 4d) when the geofluid

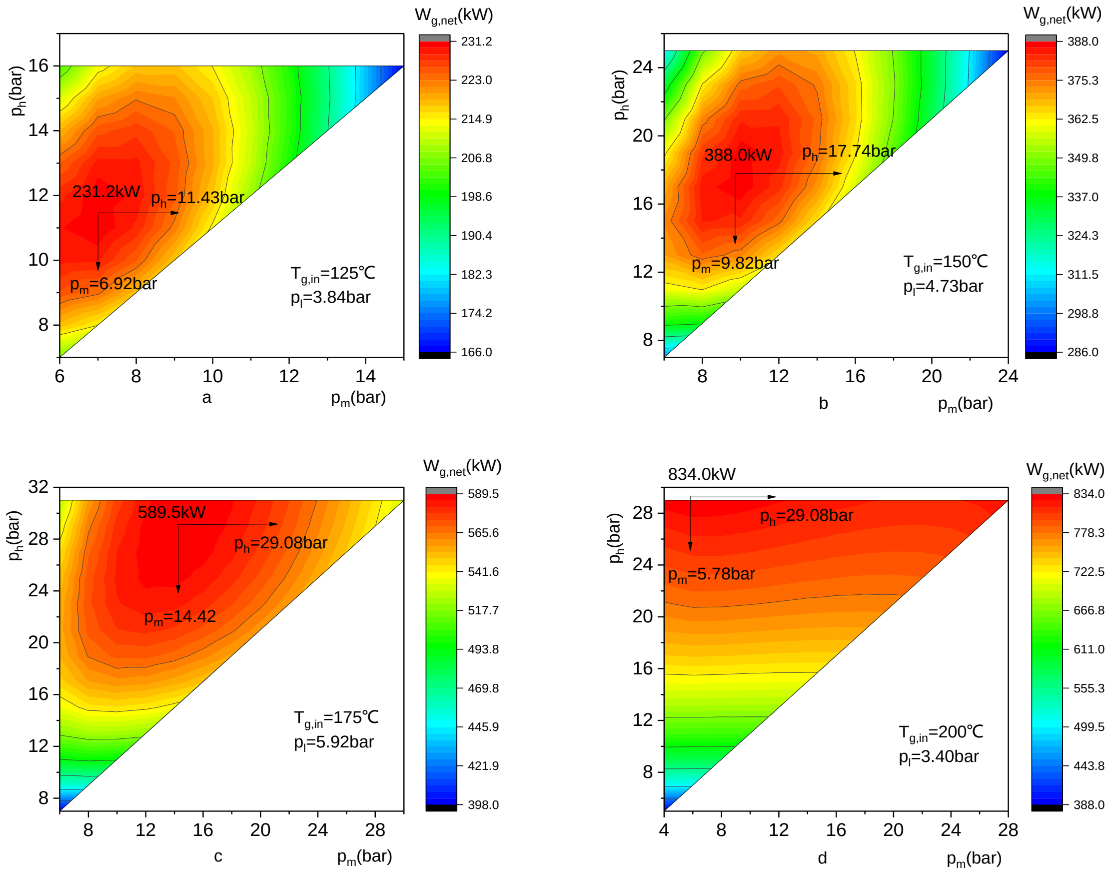

Fig.4. Optimization results of the TPORC showing the net power output contours with respect to p_h and p_m. (T_e=10°C, d_t=5°C)

Fig.4 presents the optimization results of the TPORC system. Here, the net power output was chosen as objective function, and the three pressures (p_h , p_m and p_l) were optimized simultaneously. Figures 4a, 4b, 4c, and 4d show the net power output contours with respect to p_h and p_m when the geofluid temperatures ($T_{g,in}$) are 125°C, 150°C, 175°C, and 200°C respectively.

It is seen in Fig.4 that, the optimum values (in bars) of the three pressures (p_h , p_m and p_l) are (11.43, 6.92, 3.84), (17.74, 9.82, 4.73), (29.08, 14.42, 5.92) and (29.08, 5.78, 3.40), corresponding to the maximum net power outputs of 231.2kW, 388.0kW, 589.5kW, and 834.0kW respectively. When the geofluid temperatures are 125°C, 150°C, and 175°C, the optimum values of the p_h are within the domain as can be seen in Figures 4a, 4b, and 4c. It is worth mentioning that, in this optimization, the upper limit of the p_h was set as 29.08 bar in order to have the high-pressure evaporation temperature to be 12°C lower than critical point temperature (154°C) of the working fluid R245fa. Thus, it is not difficult to

temperature is 200°C. It is also seen in Fig.4d that the change of p_m under this condition has very small influence on the net power output because the contours are almost horizontal.

The net power output contours (corresponding to the same optimized results shown in Fig.4) have been demonstrated in Fig.5 as well, but with respect to p_m and p_l. It can be seen that the gradient along constant p_m is greater than that along the constant p_l, indicating that the change of p_l has more influence than that of p_m on the net power output.

Copyright © 2019 ICAE

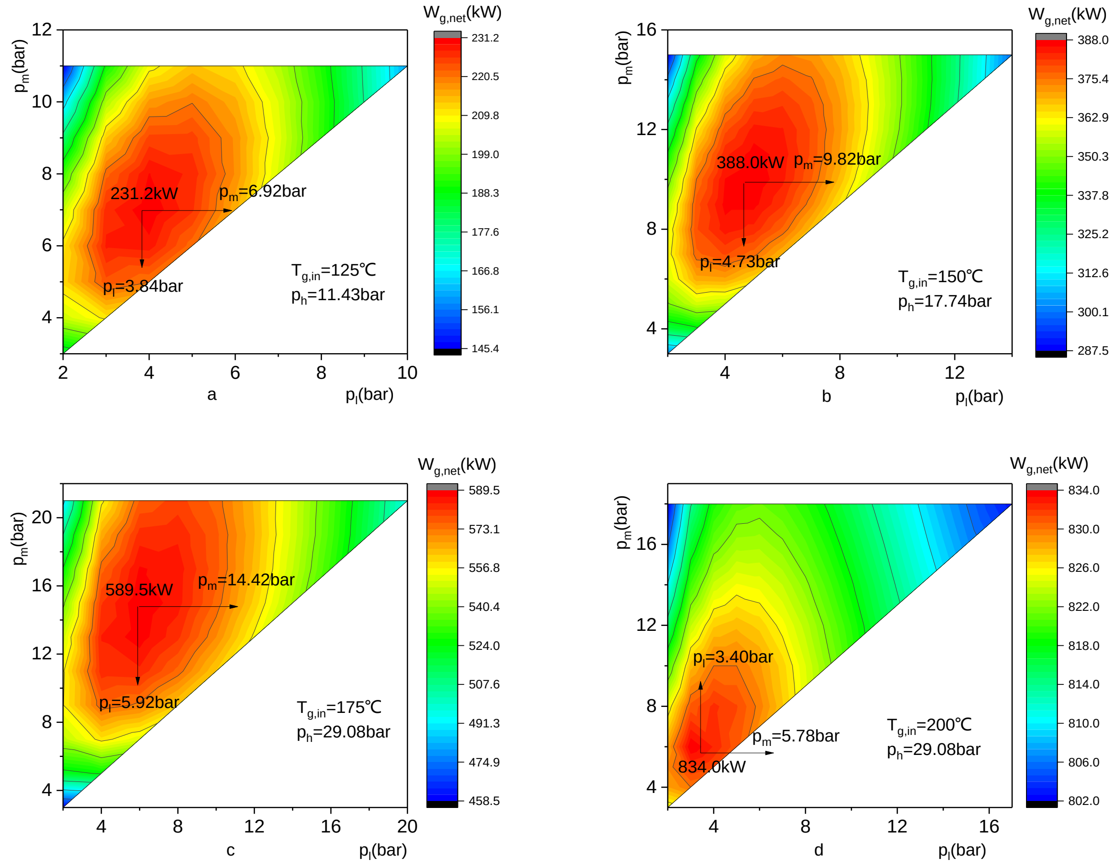

Fig.5. Optimization results of the TPORC showing the net power output contours with respect to p_m and p_l. (T_e=10°C, d_t=5°C)

4.2 Comparison among SPORC, DPORC and TPORC

Fig.6 shows the net power output comparisons among SPORC, DPORC and TPORC systems, with respect to different heat source (geofluid) temperatures. The differences of the net power output between single-pressure system (SPORC) and the multiple-pressure systems (DPORC and TPORC) decrease with the temperature increase. The net power output of the TPORC is 6.47 folds and 11.5% higher than that of the SPORC and DPORC respectively when the geofluid temperature is 135°C; whereas it is only 25.7% and 2.5% if the geofluid temperature is 170°C. When the geofluid temperature is 200°C, the difference is almost negligible, indicating that the advantage of using a multiple-pressure system diminishes as the geofluid temperature increases. In terms of using the medium-low geothermal resources (100°C -150°C), the TPORC could be a choice but further techno-economic analysis should be carried out to validate this.

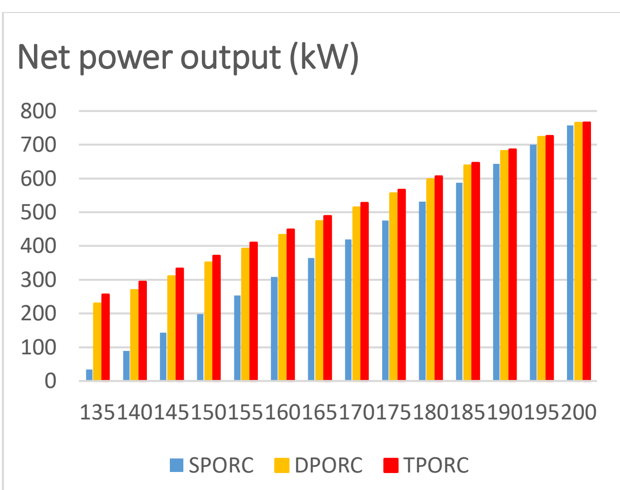

Fig.6. Net power output comparisons among SPORC, DPORC and TPORC with respect to different heat source temperatures, in kW.

5. CONCLUSIONS

The thermodynamic performance and optimization of the TPORC was investigated using R245fa as working fluid. The main conclusions can be summarized as follows:

Copyright © 2019 ICAE

(1) Either a lower value of pinch temperature difference or a lower value of superheat degree results in a higher net power output. The pinch temperature difference has more influence than the superheat degree.

(2) For a given p_h, the change of p_l has more influence than that of p_m on the net power output.

(3) With respect to the net power generation, the multiple-pressure systems show advantages over the SPORC when the geofluid temperature is low, especially when it is less than 150°C. In this case, the TPORC could be chosen for power generation for utilizing medium-low geothermal resources (100°C -150°C), but detailed analysis should be carried out to make sure that the TPORC has a sound techno-economics.

ACKNOWLEDGEMENT

This work was supported by the National Key Research and Development Program of the 13th Five-Year Plan of China (No. 2018YFB1501805).

REFERENCE

[1] Xu C, Dowd PA, Tian ZF. A simplified coupled hydro-thermal model for enhanced geothermal systems. APPL ENERG. 2015; 140:135-145.

[2] Olasolo P, Juárez MC, Morales MP, D Amico S, Liarte IA. Enhanced geothermal systems (EGS): A review. Renewable and Sustainable Energy Reviews. 2016;56:133-144.

[3] Hussain A, Arif SM, Aslam M. Emerging renewable and sustainable energy technologies: State of the art. Renewable and Sustainable Energy Reviews. 2017;71:12-28.

[4] Collings P, Yu Z, Wang E. A dynamic organic Rankine cycle using a zeotropic mixture as the working fluid with composition tuning to match changing ambient conditions. APPL ENERG. 2016;171:581-591.

[5] Liu Q, Shen A, Duan Y. Parametric optimization and performance analyses of geothermal organic Rankine cycles using R600a/R601a mixtures as working fluids. APPL ENERG. 2015;148:410-420.

[6] Kang Z, Zhu J, Lu X, Li T, Wu X. Parametric optimization and performance analysis of zeotropic mixtures for an organic Rankine cycle driven by low-medium temperature geothermal fluids. APPL THERM ENG. 2015;89:323-331.

[7] Karimi S, Mansouri S. A comparative profitability study of geothermal electricity production in developed and developing countries: Exergoeconomic analysis and optimization of different ORC configurations. RENEW ENERG. 2018;115:600-619.

[8] Manente G, Lazzaretto A, Bonamico E. Design guidelines for the choice between single and dual pressure layouts in organic Rankine cycle (ORC) systems. ENERGY. 2017; 123:413-431.

[9] Li J, Ge Z, Duan Y, Yang Z. Parametric optimization and thermodynamic performance comparison of single-pressure and dual-pressure evaporation organic Rankine cycles. APPL ENERG. 2018; 217:409-421.

[10] Li J, Ge Z, Liu Q. Thermo-economic performance analyses and comparison of two turbine layouts for organic Rankine cycles with dual-pressure evaporation. ENERG CONVERS MANAGE. 2018;164:603-614.

[11] Shokati N, Ranjbar F, Yari M. Exergoeconomic analysis and optimization of basic, dual-pressure and dual-fluid ORCs and Kalina geothermal power plants: A comparative study. RENEW ENERG. 2015;83:527-542.

[12] Du Y, Yang Y, Hu D, Hao M, Wang J, Dai Y. Off-design performance comparative analysis between basic and parallel dual-pressure organic Rankine cycles using radial inflow turbines. APPL THERM ENG. 2018;138:18-34.

[13] Guzović Z, Rašković P, Blatarić Z. The comparision of a basic and a dual-pressure ORC (Organic Rankine Cycle): Geothermal Power Plant Velika Ciglena case study. ENERGY. 2014;76:175-186.

[14] Wang M, Chen Y, Liu Q, Yuanyuan Z. Thermodynamic and thermo-economic analysis of dual-pressure and single pressure evaporation organic Rankine cycles. ENERG CONVERS MANAGE. 2018;177:718-736.

[15] Mosaffa AH, Mokarram NH, Farshi LG. Thermo-economic analysis of combined different ORCs geothermal power plants and LNG cold energy. GEOTHERMICS. 2017;65:113-125.

[16] Wang S, Liu C, Zhang C, Xu X, Li Q. Thermo-economic evaluations of dual pressure organic Rankine cycle (DPORC) driven by geothermal heat source. J RENEW SUSTAIN ENER. 2018;10:63901.

Copyright © 2019 ICAE